Nonlinearity of a composite relaxor ferroelectric transducer

Jian-yu Lu,[1] Tai K. Song,[1] James F. Greenleaf,[1] and Clyde G. Oakley[2]

[1]Biodynamics Research Unit, Department of Physiology and Biophysics, Mayo Clinic/Foundation, Rochester, MN 55905
[2]Tetrad Corporation, Englewood, CO 80111

ABSTRACT

Relaxor ferroelectric materials have been studied extensively in both theory and experiments for many years. Their applications to medical ultrasonic transducers have also been investigated. In this paper, we report an experimental study of a composite relaxor ferroelectric transducer and its nonlinear phenomenon at certain bias voltages. Novel applications of the relaxor transducer to diffraction-limited beam production, acoustic power measurement, low speckle medical imaging, and high resolution pulse-echo imaging are discussed.

1. INTRODUCTION

Relaxor ferroelectric materials[1–3] have been used for making transducers of medical and other applications.[4–9] They have high dielectric constants in the Curie range (can be used for making compact capacitors[6] or making high capacity capacitors to store electric energy), small domain size which allows the materials to be diced into fine fibers to make composite transducers for medical applications, and high displacement precision for applications such as precision mechanical movement control (electrostrictive actuators[7]).

In this paper, we report characteristics of a 1–3 composite relaxor ferroelectric transducer (composite transducers have many advantages in medical applications[10]) and their nonlinear phenomenon at certain bias voltages. Applications of the relaxor transducer to diffraction-limited beams (such as Bessel beams and X waves),[11–15] acoustic power measurement, low speckle medical imaging, and high resolution pulse-echo imaging will be discussed.

In Section 2, we show some linear properties of the composite relaxor transducer. The nonlinearity of the relaxor transducer and its comparison to linear mode will be reported in Section 3. Discussion and conclusion will be given in Sections 4 and 5, respectively.

2. RELAXOR TRANSDUCER AS A LINEAR DEVICE

One of the important applications of composite relaxor ferroelectric transducers is for medical imaging. Composite materials have lower acoustic impedance and match better to biological soft tissues. They have lower cross talk for transducer arrays because the mechanical coupling between the transducer elements is damped by bounding materials. Electromechanical coupling coefficients of composite materials are higher at certain volume fractions.[10] In the following, we will show measured

0-8194-0906-5/92/$4.00

pulse-echo waveforms of a composite relaxor transducer. Hysteresis curves (sensitivity-bias curves) and their temperature dependence will also be described.

2.1. Pulse-echo responses of relaxor transducer

Figure 1 shows a block diagram for measuring pulse-echo responses of the composite ferroelectric transducer. A function generator (WAVETEK 270) was used for remote control of a DC high voltage power supply (HP 6209B) which provided a DC bias to the transducer. The transducer was immersed in water and a one-inch thick steel block was placed 8 mm away from the surface of the transducer with its surface normal to the axis of the transducer. The broadband pulse-echo unit (PANAMETRIC 5052UA) sent a high voltage impulse (about 180 V in peak) to the transducer and echoes were amplified and recorded.

The transducer is composed of a disk-shape active composite material (volume fraction is about 30% and bounding material is epoxy) with a diameter of 4 mm and central frequency of around 6 MHz. The transducer has a backing and a front matching layer. It has two elements which were made by cutting the electrode on one side of the active material into two D shapes (see Fig. 1).

Figures 2(1) and 2(2) are pulse-echo waveforms obtained from Elements A and B of the composite relaxor transducer, respectively. Their normalized spectra are shown in Figs. 2(3) and 2(4), respectively. The transducer was biased at 200 V_{DC} at which the transducer is a linear device (linear mode). The -6 dB pulse-echo bandwidth of the transducer is about 25% of its central frequency (see Figs. 2(3) and 2(4)).

2.2. Hysteresis curves of relaxor transducer

The composite relaxor transducer presents strong hysteresis characteristics with a temperature dependence. In the following, we combine the two transducer elements into one by connecting them in parallel with a RF connector.

Figures 3(a) and 3(b) show block diagrams for measuring transmitting and receiving hysteresis curves, respectively. In Fig. 3(a), a polynomial waveform synthesizer (Model DATA 2045) generated a 20 μs, 6 MHz tone burst. The tone burst was amplified by a 50 dB ENI RF power amplifier (Model 240L) to drive the transducer via a 1 μF 400 V capacitor. DC bias voltage was supplied to the transducer through a low-pass filter to block the RF tone burst from entering the DC power supply. The transducer was immersed in a water tank and the acoustic wave emitted was measured with a 1 mm diameter hydrophone (MEDICOTEKNISK INSTITUT) that was placed on the axis of the transducer at distance Z = 180 mm. This distance is in the far field of the transducer (well beyond the Rayleigh distance, 64 mm). The sensitivity of the hydrophone at 6 MHz is about 2.041734×10^{-7} V/Pa. The received signals were sent to an oscilloscope via a buffer amplifier. The polynomial waveform synthesizer and the oscilloscope were synchronized with 1 KHz triggering pulses.

For measurements of the relaxor transducer as a receiver, a system block diagram in Fig. 3(b) was used. A 6 MHz tone burst produced from the polynomial waveform synthesizer was amplified and sent to a commercial PZT transducer (PANAMETRIC). The transducer has about 6.35 mm diameter and

a central frequency around 5 MHz. The relaxor transducer was place at distance Z = 180 mm away from the PANAMETRIC transducer which has a Rayleigh distance of about 161 mm. The axes of the two transducers were aligned with each other. The relaxor transducer was biased with the variable DC power supply and its output signals were coupled through a 1 μF 400 V capacitor with a 50 Ohm load (the RC constant is about 50 μs). Voltage across the 50 Ohm load were measured with an oscilloscope in DC coupling mode. The polynomial waveform synthesizer and the oscilloscope were synchronized with 1 KHz triggering pulses. To record the waveforms, the received signals were linearly amplified (the amplifiers have 30 MHz bandwidth), digitized, and transferred to a disk (Fig. 3(b)).

The transmitting and receiving hysteresis curves of the relaxor transducer are shown in Figs. 4(a) and 4(b), respectively. The transmitting hysteresis curves were measured at two temperatures (20 °C and 40 °C). The "rounded square" and the "diamond" symbols represent bias increase and decrease, respectively, at the points where the data were measured. The receiving hysteresis curves were obtained at one temperature (20 °C). It is seen that the curves present strong hysteresis which diminishes with increased temperature. The maximum sensitivity and the minimum sensitivity of each curve have about two-orders of magnitude difference. Therefore, the sensitivity of the relaxor transducer can be controlled with the DC bias.

3. NONLINEARITY OF A RELAXOR TRANSDUCER

During the study of the composite relaxor ferroelectric transducer, we found that the transducer presented nonlinear properties under certain biases. The biases for producing the nonlinearity are not a fixed voltage but depend on the bias history of the transducer (hysteresis). The nonlinearity usually occurs at vicinities of the valleys of the hysteresis curves but drift away slowly with time at a particular bias. Nonlinear waveforms produced from the relaxor transducer could be partially rectified RF signals and have rich harmonic components. In the following, we explore the properties of the nonlinear phenomenon and suggest their applications.

3.1. Waveforms

The nonlinear responses of the composite relaxor ferroelectric transducer to an impinging acoustic wave are shown in Fig. 5. The waveforms were measured with the experimental system in Fig. 3(b) with the transducer biased in linear or nonlinear modes. A 20 μs, 6 MHz tone burst was produced in water and the relaxor transducer was placed at 180 mm (beyond the Rayleigh distance of the wave source) away from the source to measure the field. Figures 5(1) and 5(2) are the electrical responses when the relaxor transducer was biased in linear and nonlinear modes, respectively. Figures. 5(3) and 5(4) are spectra of the waveforms in Figs. 5(1) and 5(2), respectively. It is seen that in nonlinear mode, the harmonic components of the waveforms are greatly increased. Figure 6 is the same as Fig. 5, except that a broadband pulse with about one and half cycles was used to excite the transducer

$$f(t) = Ae^{-t^2/t_0^2} \sin \omega_0 t \tag{1}$$

where A is a constant, $\omega_0 = 2\pi f_0$, $f_0 = 6MHz$, and $t_0 = 0.167\mu s$. The harmonics are also clearly seen when the transducer was biased in the nonlinear mode.

3.2. Directivity

To see if the composite relaxor ferroelectric transducer responds only to the field magnitude when biased in a nonlinear mode, we measured the directivity curves of the transducer. The results were compared to those of simulations where the transducer was assumed to be a pure full-wave rectifying device.

3.2.1. Simulations

Suppose that a plane sinusoidal wave impinges on a flat surface of a composite relaxor ferroelectric transducer at a certain angle, θ, and the transducer is circular of diameter D, and can be rotated around an axis along a diameter. At a given time,t, there is a phase change across the surface of the transducer in a direction perpendicular to the rotation axis. For a linear transducer, this phase change can cause a phase cancelation resulting in a very small amplitude of the net signal. The amplitude of the net output time signal is a function of the rotation angle, θ, which is the directivity function of the transducer. If an oscilloscope is used to observe the output signals and measure the peak-to-valley values of the waves, one obtains

$$g(\theta) = \max_{t \in T/2} \left\{ \int_{-a}^{a} dx\ A\cos\left(\omega t - \frac{2\pi x}{\lambda}\sin\theta\right) \int_{0}^{\sqrt{a^2-x^2}} dy\ 2\cos\theta \right\} - \min_{t \in T/2} \left\{ \int_{-a}^{a} dx\ A\cos\left(\omega t - \frac{2\pi x}{\lambda}\sin\theta\right) \int_{0}^{\sqrt{a^2-x^2}} dy\ 2\cos\theta \right\} \tag{2}$$

or

$$g(\theta) = \max_{t \in T/2} \left\{ \int_{-a}^{a} dx\ h(x,\theta,t) \right\} - \min_{t \in T/2} \left\{ \int_{-a}^{a} dx\ h(x,\theta,t) \right\}, \tag{3}$$

where

$$h(x,\theta,t) = 2A\cos\theta\cos\left(\omega t - \frac{2\pi x}{\lambda}\sin\theta\right)\sqrt{a^2-x^2}, \tag{4}$$

where max and min represent peak and valley of an output RF waveform (the peak and the valley can be positive or negative depending on the DC component), A is a constant, a is the radius of the transducer, x is axis along the diameter of the transducer and is perpendicular to the rotation axis, y is along the rotation axis, ω is angular frequency, λ is the wavelength in water, t is time, and T is the period of the incident wave. A plot of the directivity function, $g(\theta)$, of a linear transducer is given by dotted lines in Fig. 7.

If the transducer is nonlinear and responds to the field as a pure full-wave rectifier, the directivity function is given by

$$g(\theta) = \max_{t \in T/2} \left\{ \int_{-a}^{a} dx\ h(x,\theta,t) \right\} - \min_{t \in T/2} \left\{ \int_{-a}^{a} dx\ h(x,\theta,t) \right\}, \tag{5}$$

where

$$h(x,\theta,t) = 2A\cos\theta\left|\cos\left(\omega t - \frac{2\pi x}{\lambda}\sin\theta\right)\right|\sqrt{a^2-x^2}. \tag{6}$$

Since $h(x,\theta,t)$ in Eq. (6) is always positive, there is a DC component from the integrations in Eq. (5). If the peak-to-valley value of the waveforms is measured, the DC component will be cancelled out (this is done by the subtraction in Eq. (5)). The full line in Fig. 7 shows the directivity curve of the nonlinear transducer without the DC component. It looks like a directivity function from a transducer of higher frequency!

If the circuits are able to measure the DC component of the output of the nonlinear transducer (absolute voltage amplitude or from 0V to peak), the directivity function should be given by

$$g(\theta) = \underset{t \in T/2}{max}\left\{\int_{-a}^{a} dx\ h(x,\theta,t)\right\}, \tag{7}$$

where

$$h(x,\theta,t) = 2A\cos\theta\left|\cos\left(\omega t - \frac{2\pi x}{\lambda}\sin\theta\right)\right|\sqrt{a^2-x^2}. \tag{8}$$

The directivity function calculated from Eqs. (7) and (8) is shown with the full line in Fig. 8. The DC component is large compared to the peak-to-valley value of the RF waveform. Since the effective area of the transducer is reduced with the rotation angle, a cosine angle dependence is obtained. Because no DC component is produced by the linear transducer, the measured value of a RF waveform from 0V to peak (absolute voltage amplitude) will be the same as that from peak-to-valley (compare dotted line in Fig. 8 to dotted line in Fig. 7).

3.2.2. Experiment

The directivity curves of the composite relaxor ferroelectric transducer were measured in both linear and nonlinear modes. The peak-to-valley values of the output waveforms were measured with an oscilloscope at angle steps of 1.8°. The results are shown in Fig. 9 which are similar to those in Fig. 7 except at larger rotation angle where the noise dominated.

We have tried to measure the DC component of the output waveform of the relaxor transducer in a nonlinear mode. It has been very difficult because the output signal in nonlinear mode is very small as compared to the DC bias voltage.

4. DISCUSSION

4.1. Bias controlled devices

From the hysteresis curves (Fig. 4), it is seen that the sensitivity of the composite relaxor ferroelectric transducer can be controlled with the bias voltages. Therefore, one of the applications of the relaxor transducer could be the control of individual elements of a transducer array with bias to produce beams of particular applications (such as diffraction-limited beams). We have observed that the polarity of the bias voltage can change the phase of the output waveforms by 180°. This could be used for making a J_0 Bessel transducer[16] where the phase of alternate elements is reversed. The aperture weighting (apodization) of the Bessel transducer could also be achieved with the control of the bias voltages.

4.2. Power detection and speckle reduction

The full-wave rectifying waveform shown in Fig. 5 suggests that the relaxor transducer could be used for power detection although its sensitivity at these biases is very low. Similarly, the relaxor transducer could be used for speckle reduction in phase-insensitive medical imaging (similar to an optical detector, the transducer will respond only to the total power of the scattered waves on its large surface, no matter how complex the wave-front is distorted by the random scatterers of tissues). Acoustic lenses could be used to improve the lateral resolution.

4.3. High resolution imaging

As is seen in Fig. 7, the relaxor transducer has a sharper directivity curve when biased at nonlinear mode if the DC component is ignored. This is good for improving lateral resolution of pulse-echo medical imaging. In conventional medical imaging, transducers of higher frequency have sharper directivity curves and hence higher lateral resolution. However, higher frequency will have higher attenuation which reduces the depth of penetration of the beams. If one could transmit a lower frequency beam with a relaxor transducer biased in linear mode and receive the signal with the transducer biased in nonlinear mode, the lateral resolution of the pulse-echo imaging could be improved without using higher frequency.

4.4. Future works

The sensitivity of the nonlinear mode of the relaxor transducer studied is about 100 times (40 dB) lower than that of the linear mode. This will limit applications of the relaxor transducer to imaging where high signal-to-noise ratio is required. We will continue to study materials which could provide higher sensitivity in the nonlinear mode. The hysteresis characteristic of the relaxor transducer is also undesirable for imaging. Fortunately, at higher temperature (close to body temperature), the hysteresis is less. For testing the phase-insensitive property of the relaxor transducers in the nonlinear mode,

transducers of larger diameter will be made. Methods for measuring the DC component of the relaxor transducer in a nonlinear mode will also be studied.

5. CONCLUSION

Composite relaxor ferroelectric transducers can be used as bias controlled imaging devices. They are nonlinear at certain bias voltages providing possibilities for novel applications for low speckle imaging, power detection, and high resolution pulse-echo imaging.

6. ACKNOWLEDGMENTS

The authors thank Randall R. Kinnick for his development of a DC bias power supply which gives an output of higher than ±300 V. We appreciate Peter R. Marsh in Echo Ultrasound for measuring the pulse-echo waveforms of the relaxor transducer. The authors also appreciate the secretarial assistance of Elaine C. Quarve and the graphic assistance of Christine A. Welch. This work was supported in part by grants CA 43920 and CA54212 from the National Institutes of Health.

7. REFERENCES

1. T. R. Shrout and J. Fielding, Jr., "relaxor ferroelectric Materials," [IEEE 1990 Ultrasonics Symposium, Honolulu, HI, Dec. 4–7, 1990], *IEEE 1990 Ultrason. Symp. Proc.* 90CH2938–9, vol. 2, pp. 711–20, 1990.
2. R. Ujiie and K. Uchino, "Dynamical domain observation in relaxor ferroelectrics," [IEEE 1990 Ultrasonics Symposium, Honolulu, HI, Dec. 4–7, 1990], *IEEE 1990 Ultrason. Symp. Proc.,* 90CH2938–9, vol. 2, pp. 725–728, 1990.
3. N. Kim, W. Huebner, S. J. Jang, and T. R. Shrout, "Dielectric and piezoelectric properties of lanthanum modified lead magnesium niobate ceramics," *Ferroelectrics,* vol. 93, pp. 341–349, 1989.
4. H. Takeuchi, H. Masuzawa, C. Nakaya, and Y. Ito, "relaxor ferroelectric transducers," [IEEE 1990 Ultrasonics Symposium, Honolulu, HI, Dec. 4–7, 1990], *IEEE 1990 Ultrason. Symp. Proc.,* 90CH2938–9, vol. 2, pp. 697–705, 1990.
5. S. W. Choi, T. R. Shrout, S. J. Jang, and A. S. Bhalla, "Dielectric and pyroelectric properties in the $Pb(Mg_{1/3}Nb_{2/3})O3$—$PbTiO_3$ system," *Ferroelectrics,* vol. 100, pp. 29–38, 1989.
6. T. R. Shrout and A. Halliyal, "Preparation of lead-based ferroelectric relaxors for capacitors," *Am. Ceram. Soc. Bulletin,* vol. 66, no. 4, pp. 704–711, 1987.
7. K. Uchino, "Electrostrictive actuators: materials and applications," *Cer. Bulletin,* vol. 65, no. 8, pp. 647–652, 1986.
8. R. W. Whatmore, P. C. Osbond, and N. M. Shorrocks, "Ferroelectric materials for thermal IR detectors," *Ferroelectrics,* vol. 76, pp. 351, 1987.
9. D. A. McHenry, J. Giniewicz, S. J. Jang, A. S. Bhalla, and T. R. Shrout, "Optical properties of hot pressed relaxor ferroelectrics," *Ferroelectrics,* vol. 93, pp. 1137–1143, 1989.

10. H. L. W. Chan and J. Unsworth, "Simple model for piezoelectric ceramic/polymer 1–3 composites used in ultrasonic transducer applications," *IEEE Trans. Ultrason., Ferroelec., and Freq. Contr.*, vol. 36, no. 4, pp. 434–441, July, 1989.
11. J. Durnin, "Exact solutions for nondiffracting beams. I. The scalar theory," *J. Opt. Soc. Am.*, vol. 4, no. 4, pp. 651–654, 1987.
12. J. Durnin, J. J. Miceli, Jr., and J. H. Eberly, "Diffraction-free beams," *Physical Review Letters*, vol. 58, no. 15, pp. 1499–1501, April 13, 1987.
13. Jian-yu Lu and J. F. Greenleaf, "Pulse-echo imaging using a nondiffracting beam transducer," *Ultrasound Med. Biol.* vol. 17, no. 3, pp. 265–281, May, 1991.
14. Jian-yu Lu and J. F. Greenleaf, "Ultrasonic nondiffracting transducer for medical imaging," *IEEE Trans. Ultrason., Ferroelec., Freq. Contr.*, vol. 37, no. 5, pp. 438–447, Sept., 1990.
15. Jian-yu Lu and J. F. Greenleaf, "Nondiffracting X waves — exact solutions to free-space scalar wave equation and their finite aperture realizations," *IEEE Trans. Ultrason., Ferroelec. Freq. Contr.*, vol. 39, no. 1, pp. 19–31, Jan., 1992.
16. Jian-yu Lu and J. F. Greenleaf, "Diffraction-limited beams and their applications for ultrasonic imaging and tissue characterization," [SPIE's 1992 International Symposium on Optical Applied Science and Engineering, San Diego, CA, July 19–24, 1992], *New Developments in Ultrasonic Transducers and Transducer Systems*, F. L. Lizzi, Editor, 1992 (Invited paper).

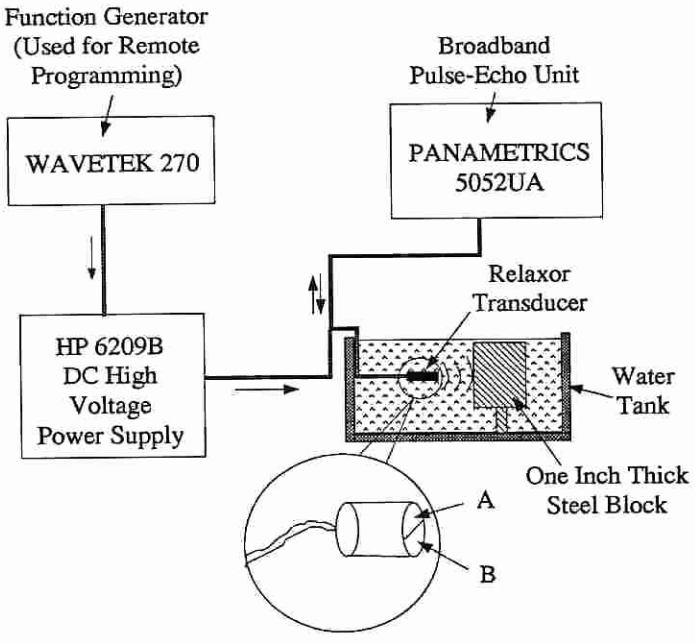

Figure 1. System block diagram for measuring pulse-echo waveforms of a relaxor transducer.

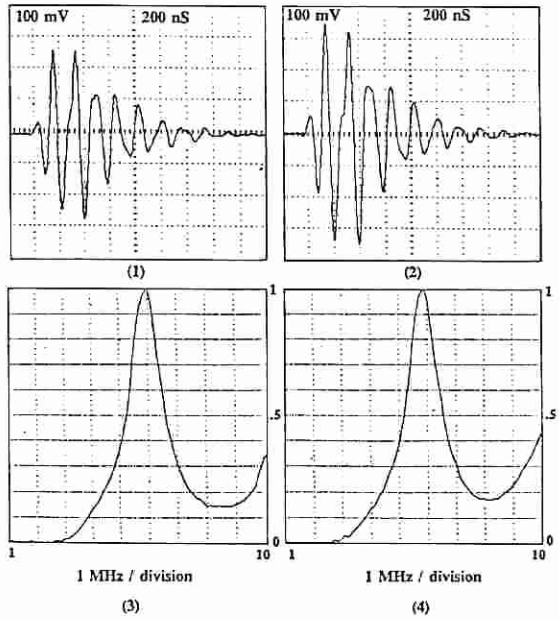

Figure 2. Pulse-echo waveforms and their spectra measured with the system in Fig. 1 and with a bias of 200 V. Panels (1) and (2) are waveforms and (3) and (4) are their corresponding spectra. 100 mV and 200 ns represent 100 mV/div and 200 ns/div as used for conventional oscilloscope. The central frequency of the spectra is about 6 MHz.

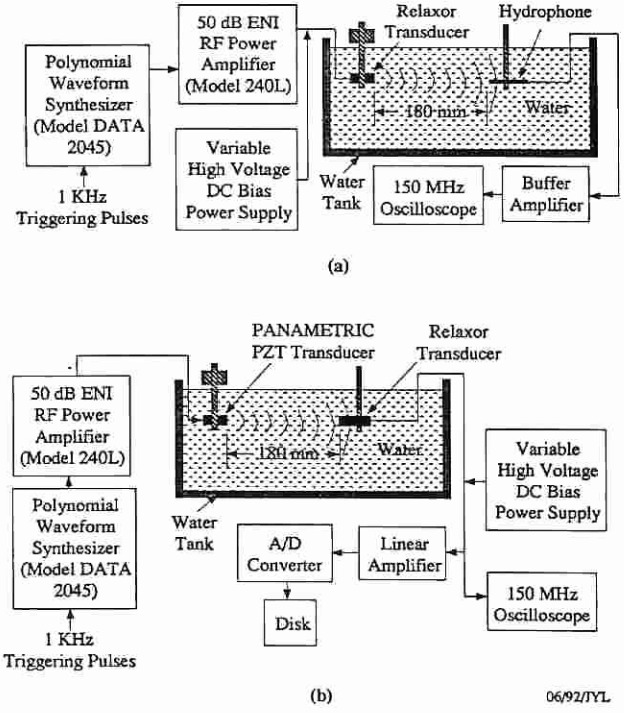

Figure 3. (a) and (b) are system block diagrams for measuring transmitting and receiving properties of the relaxor transducer, respectively.

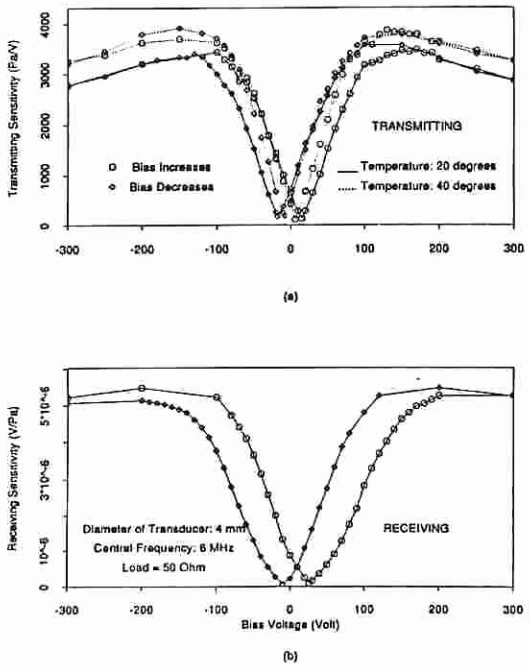

Figure 4. (a) and (b) are transmitting and receiving hysteresis curves of relaxor transducer, respectively. Full line represents results obtained at temperature of 20 °C and dotted lines the results at 40 °C. The transducer is of diameter of 4 mm and a central frequency of 6 MHz. "Rounded square" and "diamond" symbols represent points where data were measured and represent bias increasing and decreasing, respectively.

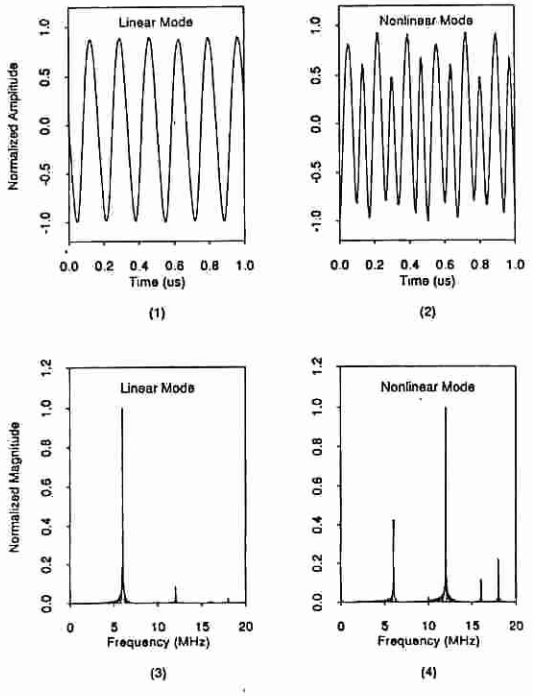

Figure 5. Received CW waveforms with the relaxor transducer biased in linear (1) and nonlinear (2) modes, respectively. Panels (3) and (4) are spectra corresponding to Panels (1) and (2), respectively.

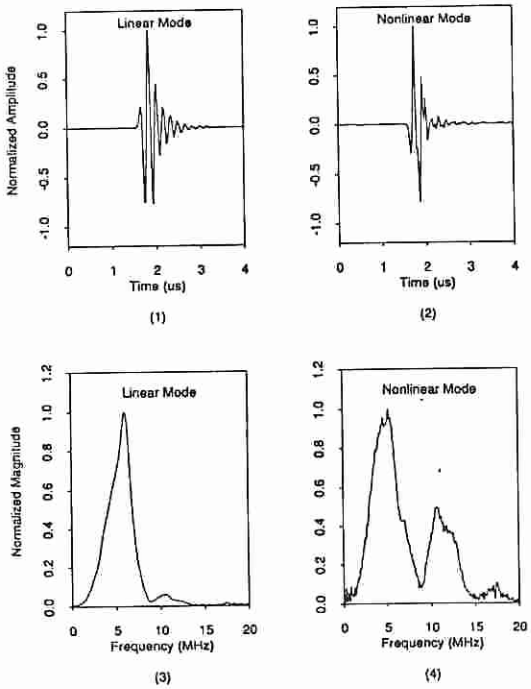

Figure 6. The same as Fig. 5, except that a one-and-half cycle pulse was used to excite the relaxor transducer.

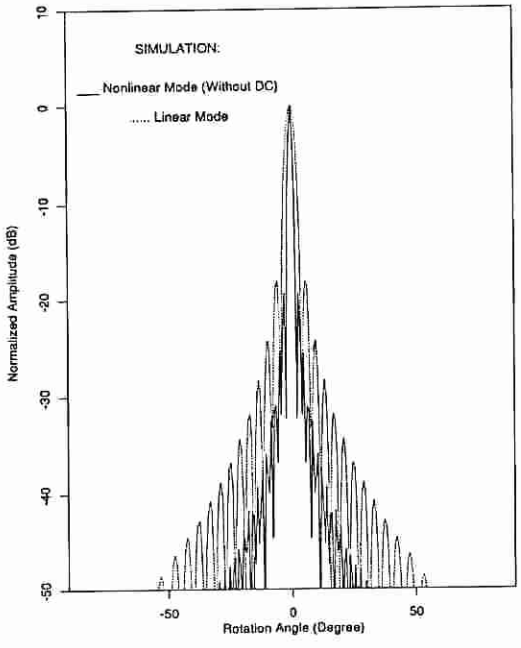

Figure 7. Simulated directivity curves of a relaxor transducer biased in linear (dotted line) and nonlinear (full line) modes. The DC component of the output of the transducer is excluded. Peak-to-valley values of the output waveforms were used for the plots.

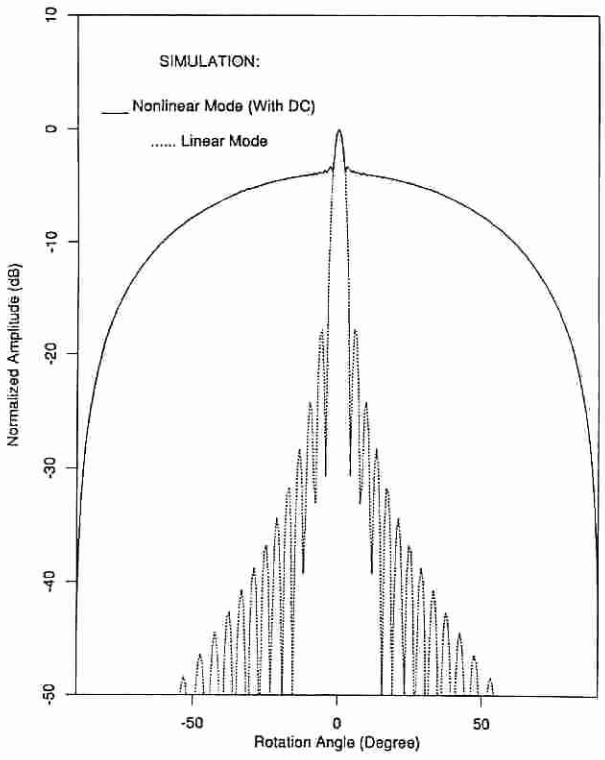

Figure 8. The same as Fig. 7, except that DC component of the relaxor transducer is included.

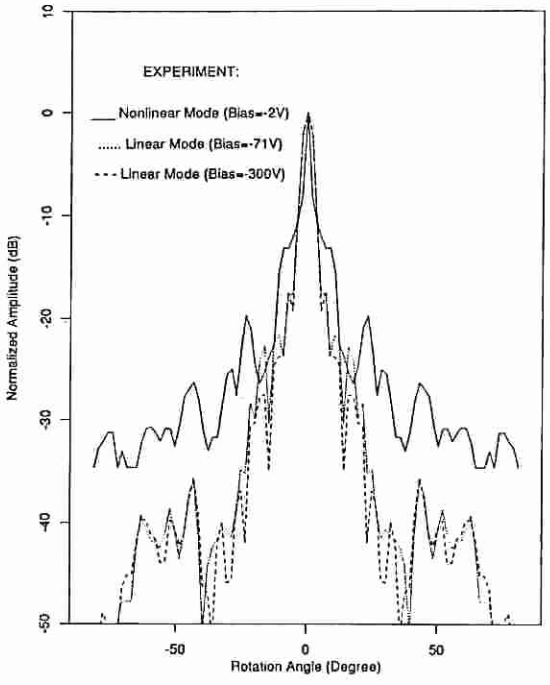

Figure 9. Measured directivity curves when the relaxor transducer was biased in linear modes (dotted and dashed lines) and nonlinear mode (full line). Peak-to-valley values of the output waveforms were measured and used for the plots.